J Mol Med (2015) 93:663–674
DOI 10.1007/s00109-015-1251-9

JMolMed

ORIGINAL ARTICLE

Carvedilol improves biventricular fibrosis and function in experimental pulmonary hypertension

Kenichi Okumura · Hideyuki Kato · Osami Honjo · Siegfried Breitling · Wolfgang M. Kuebler · Mei Sun · Mark K. Friedberg

Received: 23 July 2014 / Revised: 15 December 2014 / Accepted: 6 January 2015 / Published online: 18 January 2015

Abstract
Left ventricular (LV) function influences outcomes in right ventricular (RV) failure. Carvedilol reduces mortality in LV failure and improves RV function in experimental pulmonary arterial hypertension (PAH). However, its impact on ventricular-ventricular interactions and LV function in RV afterload is unknown. We investigated effects of carvedilol on biventricular fibrosis and function in a rat model of persistent PAH. Rats were randomized into three groups: Sham controls, PAH, and PAH+carvedilol. Severe PAH was induced by 60 mg/kg subcutaneous monocrotaline. In the treatment group, oral carvedilol (15 mg/kg/day) was started 2 weeks after monocrotaline injection and continued for 3 weeks until the terminal experiment. Echocardiography and exercise performance were performed at baseline and repeated at the terminal experiment with hemodynamic measurements. LV and RV myocardium were analyzed for hypertrophy, fibrosis, and molecular signaling by protein and mRNA analysis. PAH and PAH+carvedilol rats experienced severely elevated pulmonary arterial pressures and RV hypertrophy. Despite similar RV systolic pressures, carvedilol reduced biventricular collagen content (RV fibrosis area; 13.4±6.5 vs. 5.5±2.7 %, $p<0.001$) and expression of transforming growth factor-β1 (TGFβ1) (RV TGFβ1/glyceraldehyde 3-phosphate dehydrogenase (GAPDH) ratio; 1.16±0.39 vs. 0.57±0.22, $p<0.01$) and connective tissue growth factor (CTGF) (RV CTGF/GAPDH ratio; 0.49±0.06 vs. 0.35±0.17, $p<0.05$). RV pro-apoptotic caspase-8 was increased in PAH compared to controls and was significantly reduced in both ventricles compared to PAH animals by carvedilol. Tissue effects were accompanied by improved biventricular systolic and diastolic performance and exercise treadmill distance (36±30 vs. 80±33 m, $p<0.05$). In RV pressure-load, carvedilol improves biventricular fibrosis and function through abrogation of TGFβ1-CTGF signaling.

Key message
- RV afterload caused biventricular injury and dysfunction through TGFβ1-CTGF signaling.
- Carvedilol reduced biventricular TGFβ1-CTGF signaling, fibrosis, and apoptosis.
- Carvedilol improved cardiac output and biventricular function.
- Improved fibrosis and hemodynamics occurred despite persistent RV afterload.

Keywords Pulmonary arterial hypertension · Adrenergic receptor blocker · Right heart dysfunction · Ventricular-ventricular interactions

K. Okumura · H. Kato · O. Honjo · M. Sun · M. K. Friedberg
The Labatt Family Heart Center, Division of Cardiology and Cardiovascular Surgery, Hospital for Sick Children and University of Toronto, Toronto, ON, Canada

S. Breitling · W. M. Kuebler
The Keenan Research Center of the Li Ka Shing Knowledge Institute, St. Michael's Hospital, Toronto, ON, Canada

M. K. Friedberg (✉)
Division of Cardiology, Hospital for Sick Children, 555 University Avenue, Toronto, ON M5G 1X8, Canada
e-mail: mark.friedberg@sickkids.ca

Introduction

Ventricular-ventricular interactions refer to the cumulative effect of changes in filling, geometry, and function of one ventricle on the filling, geometry, and function of the contralateral ventricle. In pulmonary arterial hypertension (PAH), the importance of left ventricular (LV) function, through adverse ventricular-ventricular interactions, is increasingly recognized [1]. Hence, therapies

supporting biventricular function may be a useful addition to therapies that reduce right ventricular (RV) afterload [1, 2].

Prolonged RV systolic duration, expressed as the systolic-to-diastolic (*S*/*D*) duration ratio, reflects one aspect of temporal RV-LV interactions in PAH and is associated with mortality [3, 4]. The *S*/*D* ratio worsens with increasing heart rates, as diastole shortens exponentially [4]. The prolonged RV systole and increased *S*/*D* ratio impede on LV diastole further worsening adverse RV-LV interactions and biventricular myocardial injury [5, 6]. We previously demonstrated that isolated RV afterload leads not only to RV but also LV fibrosis through transforming growth factor (TGFβ1)-connective tissue growth factor (CTGF) axis signaling [5, 6].

Hence, slowing heart rate to modulate adverse ventricular-ventricular interactions, in addition to counteracting sympathetic activity may be therapeutic [7]. Indeed, previous animal studies demonstrated that β-blockade, especially carvedilol, improves RV fibrosis and function in rat PAH models [8]. However, β-blockers remain relatively contraindicated in PAH due to concerns for decreased cardiac output. Likewise, their effects on LV function and fibrosis remain unknown. We hypothesized that in PAH, carvedilol ameliorates biventricular TGFβ1-CTGF signaling to improve biventricular fibrosis and function. Accordingly, we aimed to investigate carvedilol effects on LV and RV TGFβ1-CTGF signaling, fibrosis, and function, during persistently increased RV afterload in a rat PAH model.

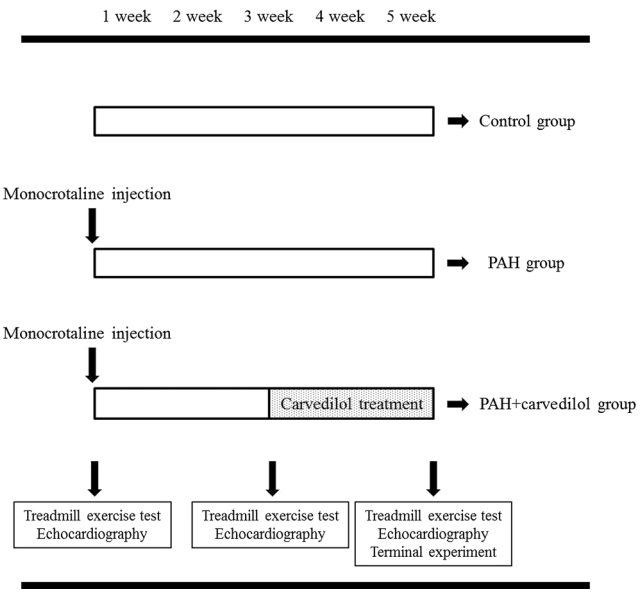

Fig. 1 Study protocol. After 2-week acclimatization to the treadmill, 6-week-old male rats were randomly allocated into 3-groups: 1. Sham controls were given a single subcutaneous injection of 0.9 % saline. 2. The PAH group were given a single subcutaneous injection of 60 mg/kg monocrotaline to induce severe PAH; and 3. the PAH+carvedilol group were started on carvedilol (15 mg/ kg/ day) 2 weeks after monocrotaline injection for a duration of 3 weeks until the terminal experiment. Treadmill exercise endurance and echocardiography were performed at baseline, before carvedilol, and before the terminal experiment. *PAH* pulmonary arterial hypertension

Methods

Protocol

The experimental protocol (Fig. 1) was approved by the institutional Animal Ethics Committee. Six-week-old male Sprague-Dawley rats (Charles River, Canada) weighing 231 ±20 g at protocol onset were randomly allocated into three groups: (1) Sham controls received a single subcutaneous injection of 0.9 % saline (3 mL/kg); (2) positive controls received a single subcutaneous injection of 60 mg/kg monocrotaline (3 mL/kg); and (3) the treatment group received oral carvedilol (15 mg/kg/day) 2 weeks after monocrotaline injection for 3 weeks until the terminal experiment.

Exercise endurance

Animals were acclimatized to a treadmill (Exer 3/6, Columbus Instruments, OH) for 2 weeks before monocrotaline. Treadmill endurance (15° inclination; 10 m/min), measured by the distance ran until exhaustion (established when rats accepted three consecutive mild (1.2 mA) electric stimuli) was performed before monocrotaline and before the terminal experiment.

Echocardiography

Rats were imaged under 3 % isoflurane sedation (275 frames/s; 12-MHz transducer Vivid E9, General Electric, Wauwatosa). M-mode and 2D short-axis views at the papillary-muscle level and apical four-chamber view were acquired. Strain was analyzed using GE EchoPac, version 8.0.

The fractional area change (FAC) was calculated as end-diastolic – end-systolic area/end-diastolic RV area [4]. Echo parameters included tricuspid inflow early (*E*) and late (*A*) velocities, tricuspid lateral annulus tissue Doppler imaging (TDI) (systolic velocity (*S*′), early (*E*′), and late (*A*′) diastolic velocities, isovolumic relaxation (IVRT), contraction (ICT) and ejection times (ET), *E*/*E*′ ratio), RV myocardial performance index (MPI) [9] (a parameter of global cardiac function), and the *S*/*D* duration ratio from TR Doppler and TDI [4, 10]. The interval from cessation to the onset of RV inflow (*a*) and RV ejection time (*b*) were measured. MPI was calculated as $(a-b)/b$ [9].

Global RV longitudinal and LV longitudinal, radial, and circumferential strain were derived from 2-D speckle tracking. Adequate tracking was visually verified and manually corrected as necessary [11].

Interobserver and intraobserver variability were evaluated using the coefficient of variation [12].

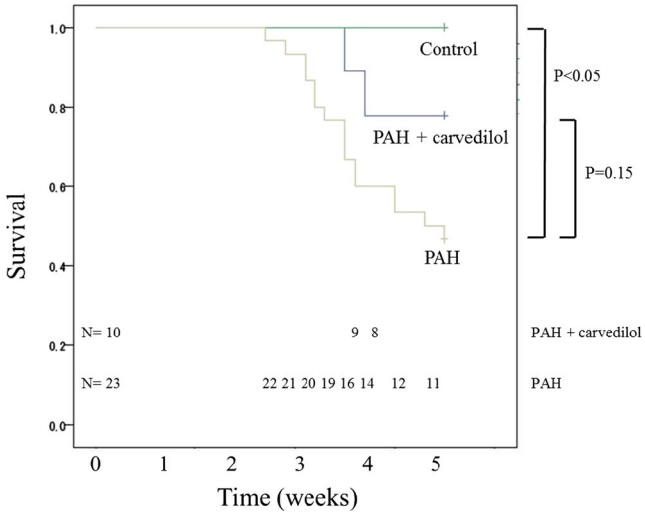

Fig. 2 Kaplan-Meier survival of controls (n=8), PAH (n=23), and PAH+carvedilol rats (n=10). *PAH* pulmonary arterial hypertension, *CAR* carvedilol

Hemodynamics

At the terminal experiment, hemodynamics were measured following echocardiography. After thoracotomy, a 2F conductance catheter (Millar Instruments, Houston) was inserted into the RV apex and heart rate, stroke volume, cardiac output, end-systolic and diastolic volumes, and pressures were determined from pressure-volume loops. The maximal rate of ventricular pressure rise and decay (dp/dt max, dp/dt min) were calculated. Tau was assessed as the time constant of mono-exponential decay of ventricular pressure during isovolumic relaxation [13]. Myocardial contractility (elastance, Ees) was determined from a family of pressure-volume loops recorded during transient occlusion of the inferior vena cava [13]. After measuring RV hemodynamics, the catheter was inserted through the LV apex to measure LV hemodynamics.

To study chronic carvedilol effects on acute adrenergic response in PAH, we assessed RV hemodynamics after 10 min of rest; and with incremental IV dobutamine (5, 10, and 20 μg/kg/min for 5 min) and esmolol (200 μg/kg/min for 15 min) given through the tail vein, in random order, at least 15 min apart, and after heart rate normalized.

Table 1 Carvedilol effects on body and cardiac weight, heart rate, and exercise endurance

	Control (n=8)	PAH (n=7)	PAH+carvedilol (n=8)
BW (g)	479±46	384±43**	418±64
RV (mg)	268±23	547±82***	506±54***
RV/BW (mg/g)	0.56±0.05	1.44±0.25***	1.19±0.22***, †
LV+IVS (mg)	968±13	868±9	915±20
LV+IVS/BW (mg/g)	1.99±0.12	2.12±0.18	2.19±0.15†
RV/LV+IVS ratio	0.28±0.03	0.68±0.1***	0.55±0.12***, †
HR (bpm)	349±31	359±54	296±20**, ††
Treadmill distance (m)	81±32	36±30*	80±33†

PAH pulmonary arterial hypertension, *BW* body weight, *RV* right ventricle, *LV+IVS* left ventricle (LV)+interventricular septum (IVS), *HR* heart rate

*p<0.05, **p<0.01, ***p<0.001 vs. control rats; †p<0.05, ††p<0.01 vs. PAH rats

Table 2 Invasive hemodynamic and functional parameters

	Control (n=8)	PAH (n=7)	PAH+carvedilol (n=8)
SV (mL)	0.36±0.2	0.13±0.14**	0.26±0.14†
CO (mL/min)	104±61	29±19***	64±38†
RV peak systolic pressure (mmHg)	23±2	50±20**	57±29**
RV end-diastolic pressure (mmHg)	1.7±1.2	3.6±2.7*	1.5±1.2†
RV dP/dt max (mmHg/s)	1,012±398	1,463±566	2,119±789**, †
RV dP/dt min (mmHg/s)	−741±165	−1,286±633	−1,927±999**, †
RV Ees (mmHg/mL)	56±39	49±36*	110±67†
RV Tau (ms)	14±4	34±16*	15±3†
LV peak systolic pressure (mmHg)	78±14	56±22	70±25
LV end-diastolic pressure (mmHg)	3.9±0.7	3.8±4.2	2.5±1.4
LV dP/dt max (mmHg/s)	3,196±618	1,914±1,022*	3,350±1,544 ††
LV dP/dt min (mmHg/s)	−2,650±650	−1,225±675*	−2,329±1,453†
LV Ees (mmHg/mL)	289±344	134±205	462±550
LV Tau (ms)	12±2	29±12**	15±4†
RVp/LVp	0.31±0.08	0.95±0.33**	0.85±0.32**

PAH pulmonary arterial hypertension, *SV* stroke volume, *CO* cardiac output, *RV* right ventricle, *Ees* end-systolic elastance

*p<0.05, **p<0.01, vs. control rats; †p<0.05, ††p<0.01 vs. PAH rats

Tissue analysis

Following hemodynamics, the lungs and heart were harvested. RV and LV+septum (IVS) were weighed. Tissues were snap-frozen and stored at −80°C for protein analysis. A second sample was fixed in 10 % neutral-buffered formaldehyde and embedded in paraffin. The lungs were perfused with formalin via the trachea before they were harvested. Five-micrometer cross-sections were stained with hematoxylin-eosin (HE) and picrosirius red F3BA (PSR) for morphology and interstitial collagen content expressed as a percentage of the total collagenous and non-collagenous areas (Adobe Photoshop CS2, San Jose, CA). Cardiomyocyte diameter

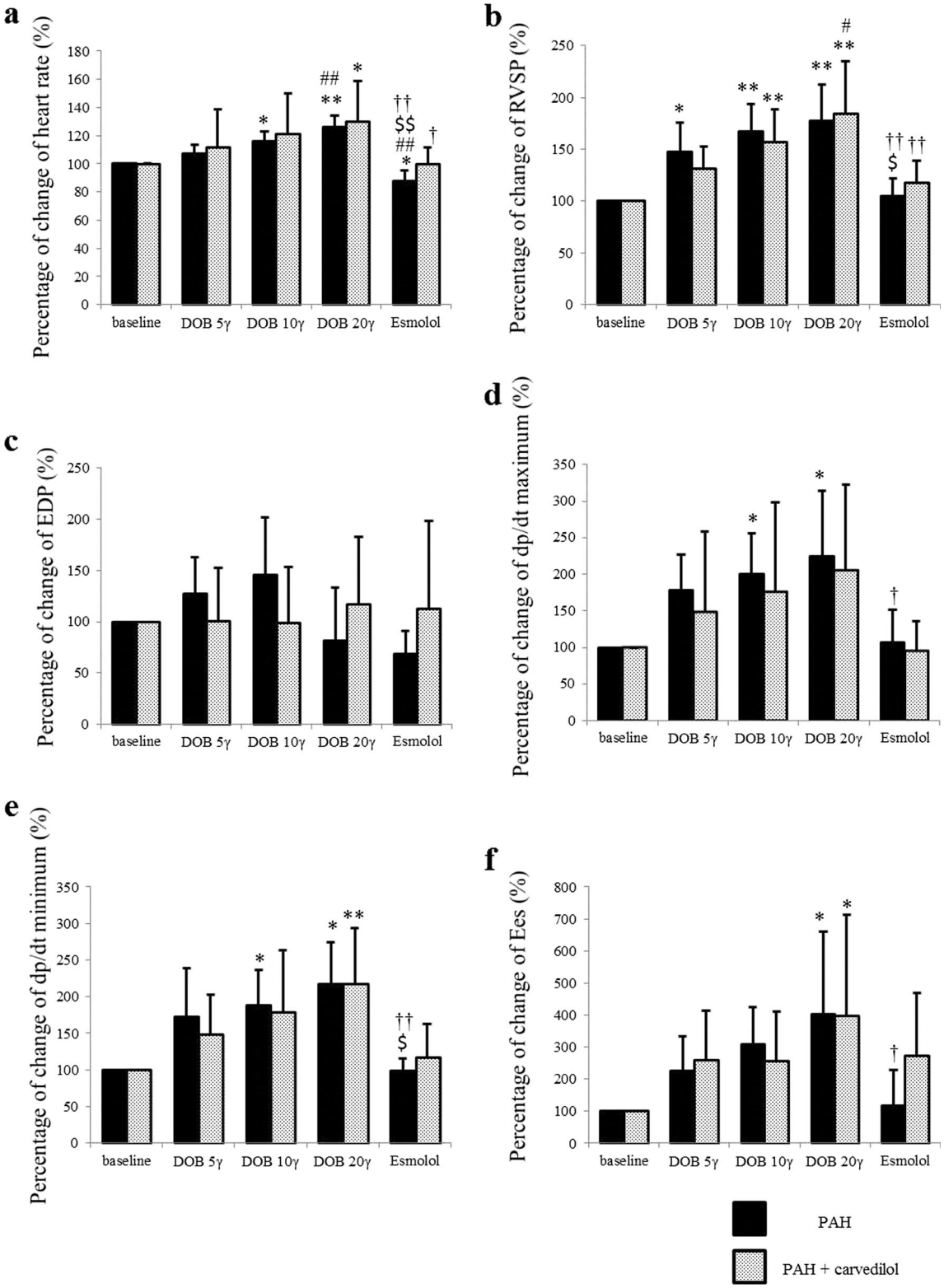

Fig. 3 Effects of stepwise increasing doses of dobutamine (*DOB*) and esmolol on RV hemodynamics expressed as the percentage of change from baseline in PAH (n=3) and PAH+carvedilol groups (n=5). *RVSP* right ventricular systolic pressure, *EDP* end-diastolic pressure, *Ees* end-systolic elastance. *p<0.05, **p<0.01 vs. baseline in each group, #p<0.05, ##p<0.01 vs. DOB 5γ, \$$p$<0.05, \$\$$p$<0.01 vs. DOB 10γ, †$p$<0.05, ††$p$<0.01 vs. DOB 20γ

Table 3 Echocardiography parameters of right and left ventricular function

	Control (n=8)	PAH (n=7)	PAH+carvedilol (n=8)
LVEDD (mm)	8.6±1.2	6±0.1***	6.7±0.1*
LVEF (%)	69±8	67±7	77±7†
RVEDD (mm)	2.7±0.7	4.3±0.9**	4.7±1***
FAC (%)	42±6	32±10*	35±7
TAPSE (mm)	2.7±0.4	1.7±0.4***	2.1±0.3**, †
RV MPI	0.11±0.09	0.44±0.24*	0.34±0.18
TDI analysis			
LV S' (cm/s)	7.3±1	4.5±0.5**	6.6±1.8††
LV TDI derived S:D ratio	1.03±0.19	1.44±0.22**	1.12±0.23†
RV S' (cm/s)	6.5±1.3	4.3±1*	6.1±1.6†
RV TDI derived S:D ratio	1±0.11	1.55±0.24***	1.16±0.16†††
RV TDI derived MPI	0.32±0.07	0.54±0.06**	0.36±0.11††
Strain analysis			
LV radial strain (%)	28.6±7.6	16.2±9.5**	24.1±6.2†
LV circumferential strain (%)	−16±2.8	−10.4±3.8**	−10.4±2.4**
LV longitudinal strain (%)	−14.9±1	−10.4±4.4*	−10.2±2.9*
RV longitudinal strain (%)	−16.5±1.8	−8.5±2.8***	−11.7±3.6**, ††

PAH pulmonary arterial hypertension, *LVEDD* left ventricular (LV) end-diastolic diameter, *LVEF* left ventricular ejection fraction, *RVEDD* right ventricular (RV) end-diastolic diameter, *FAC* fractional area change, *TAPSE* tricuspid annular plane systolic excursion, *MPI* myocardial performance index, *TDI* tissue Doppler imaging, S' systolic velocity of atrioventricular valve, *S:D ratio* the ratio of systolic duration (S) to diastolic duration (D)

*p<0.05, **p<0.01, ***p<0.001 vs. control rats; †p<0.05, ††p<0.01 †††p<0.001 vs. PAH rats

was measured from HE-stained sections using National Institutes of Health ImageJ software (http://rsweb.nih.gov/ij/). Lungs were stained with HE to assess for monocrotaline-induced injury, blinded to group allocation, using an established histological score from 0 (no injury) to 1 [14].

Myocarditis severity was scored as described previously to assess for monocrotaline-induced myocarditis treated by carvedilol using a semiquantitative scale: 0, no inflammatory infiltrates; 1, small foci of inflammatory cells between myocytes; 2, larger foci of >100 inflammatory cells; 3, >10 % of a cross-section involved; 4, >30 % of a cross-section involved [15].

Protein was extracted from freshly prepared or snap-frozen myocardium using standard methodology [16]. Membranes were incubated with transforming growth factor β1 (TGFβ1), CTGF (Abcam, Cambridge, MA), Smad 2,3, and 4, p-38 MAPK, phospho p-38 MAPK, caspase-3, caspase-8 (Cell Signaling Technology Inc., Danvers, MA), β1 and β2-adrenergic receptor antibodies (Abcam), protein kinase A (PKA) (Cell Signaling Technology), cardiac sarcoplasmic reticulum Ca^{2+} ATPase (SERCA2a) (Sigma, St. Louis, MO), and glyceraldehyde 3-phosphate dehydrogenase (GAPDH) (Abcam). Gelatinolytic activities of MMP-2 and MMP-9 were examined to reflect extracellular matrix (ECM) remodeling.

Statistics

All results including exercise endurance, echocardiography, hemodynamic measurements, histology, protein, and gelatin zymography analysis were obtained from animals surviving to the end of the protocol. Data are expressed as mean±standard deviation. Comparisons were made by one-way analysis of variance (ANOVA) with Bonferroni post hoc testing. A p value <0.05 was considered significant. Analysis was blinded to group allocation.

Results

Twenty-three rats were studied (8 shams; 7 PAH; 8 PAH+carvedilol). Survival to protocol end in the PAH group was significantly decreased compared with shams (100 vs. 50 %, control vs. PAH, p<0.05). Carvedilol trended to improve survival but did not reach statistical significance (50 vs. 80 %, PAH vs. PAH+carvedilol, p=0.15; Fig. 2). There were no differences at baseline and at 2 weeks after monocrotaline injection in body weight, heart rate, maximal treadmill distance, and echo (data not shown). Table 1 shows biometrical characteristics at the terminal experiment. Body weight decreased significantly in PAH animals compared with controls, which was unchanged with addition of carvedilol. RV weight, RV/LV+IVS ratio, and RV/BW ratio in PAH animals were markedly increased compared with controls. RV/LV+IVS ratio and RV/BW ratio improved with carvedilol. Heart rate in the PAH+carvedilol group was significantly decreased compared with controls and PAH animals.

Exercise endurance

Maximal treadmill distance in the PAH group was decreased compared to controls (81±32 vs. 36±30 m, p<0.05) and improved with carvedilol (36±30 vs. 80±33 m, PAH vs. PAH+carvedilol, p<0.01; Table 1).

Hemodynamics

Hemodynamics and function are summarized in Table 2. RV peak systolic pressure and RV/LV systolic pressure ratio were increased in PAH and PAH+carvedilol groups vs. controls and not different between PAH and PAH+carvedilol animals.

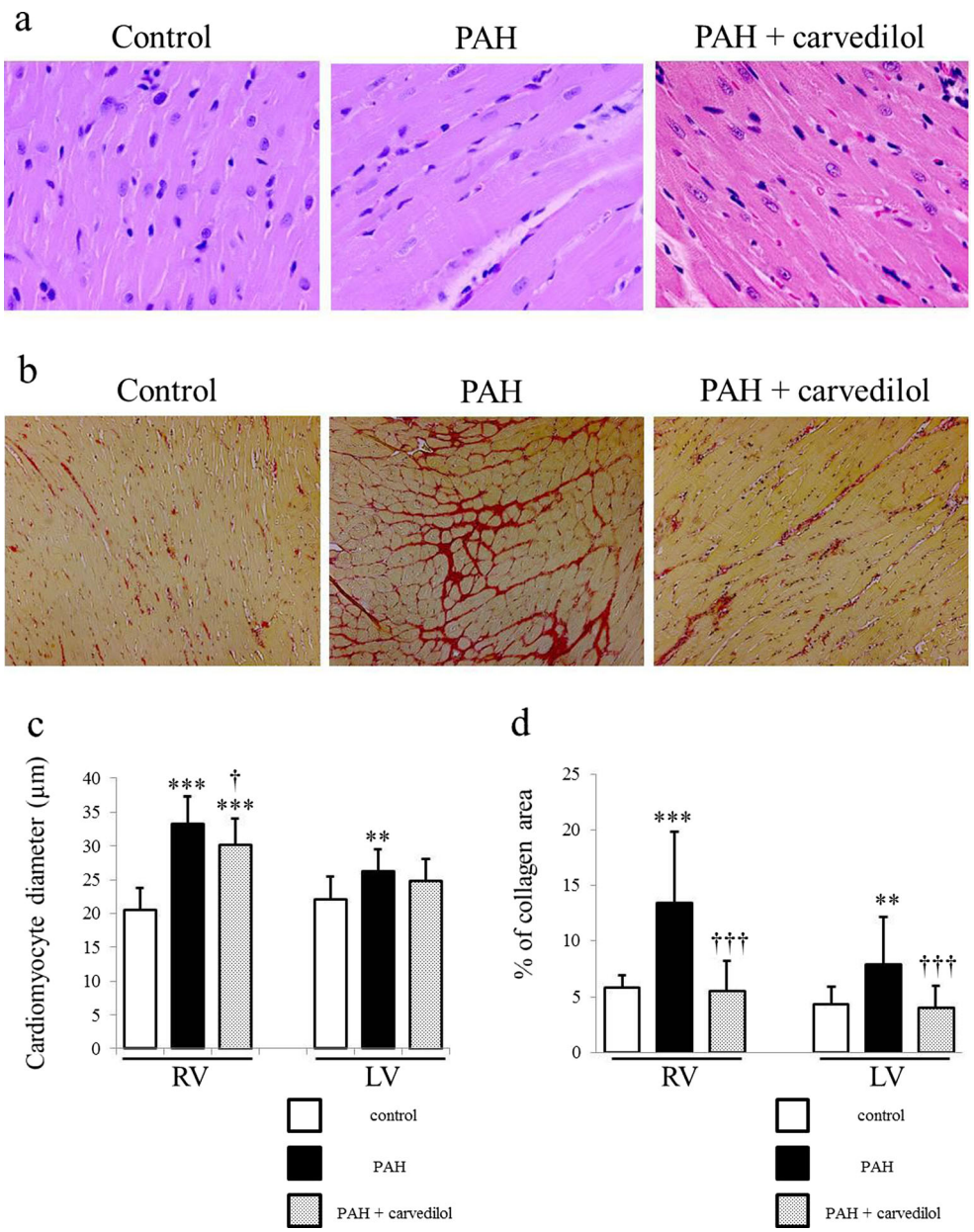

Fig. 4 Carvedilol decreases right, but not left ventricular cardiomyocyte hypertrophy induced by pulmonary arterial hypertension (*PAH*). Representative sections from the right ventricle of control (n=8), PAH (n=7), PAH+carvedilol (n=8) rats are shown in panel **a** and quantified for the right and left ventricles in panel **c**. Original magnification ×400. Carvedilol markedly reduces right and left ventricular fibrosis induced by pulmonary arterial hypertension (PAH). Representative sections from the right ventricle of controls (n=8), PAH (n=7), PAH+carvedilol rats (n=8) are shown in panel **b** and quantified for the right and left ventricles in panel **d**. Interstitial collagen was identified in picrosirius red F3BA (*PSR*) stained sections by its red appearance. Original magnification ×100

SV, CO, and LV dP/dt max were significantly decreased in PAH vs. controls and improved with carvedilol. RV dP/dt max was not statistically different between controls and PAH; while carvedilol increased RV dP/dt max and Ees compared with PAH.

Diastolic parameters including RV and LV dP/dt min and tau were significantly improved in PAH+carvedilol animals vs. PAH. There were no differences in RV and LV end-diastolic pressures and LV Ees between groups.

Figure 3a–d illustrates the percent change in hemodynamic parameters from baseline in response to acute administration of dobutamine and esmolol in PAH and PAH+carvedilol groups. Both groups responded to dobutamine infusion with HR acceleration and increased RV systolic pressure, RV dp/dt max, dp/dt min, and Ees compared with baseline. Esmolol infusion decreased HR, RV systolic pressure, dp/dt maximum, dp/dt minimum, and Ees with no significant differences between groups.

Table 3 summarizes echo results. RV end-diastolic diameter (RVEDD) in the PAH and PAH+carvedilol groups was significantly increased, while LV end-diastolic diameters in the PAH and PAH+carvedilol groups were reduced vs. controls. Carvedilol did not change RV or LV dimensions vs. PAH, while LVEF improved. RV FAC and tricuspid annular plane systolic excursion (TAPSE) were significantly reduced in the PAH group vs. controls. Carvedilol improved TAPSE, albeit to less than control values, without change in FAC. RV MPI in the PAH group was increased vs. controls and lower with carvedilol although not statistically significant.

TDI parameters including LV and RV *S′*, LV, and RV TDI derived *S/D* ratio and RV TDI derived MPI were worse in PAH vs. controls and improved with carvedilol. There were no other differences in TDI parameters among the groups. LV longitudinal, circumferential, and radial strain and RV longitudinal strain were significantly reduced in PAH animals vs. controls. Carvedilol improved global LV radial and RV longitudinal strain.

Intraobserver and interobserver correlation coefficients for RV strain in the PAH group were 0.76 and 0.63, respectively. The average relative difference between intraobserver and interobserver measurements were 28.4 and 23.5 %, respectively.

Myocardial infiltration score and lung injury score

There were no significant differences among groups in the myocardial infiltration score (control vs. PAH vs. PAH+carvedilol; RV 0.33±0.58 vs. 0.86±0.69 (p=0.29 vs. control) vs. 0.86±0.69 (p=0.29 vs. control, p=1.0 vs. PAH); LV 0 vs. 0.83±0.75 (p=0.11 vs. control) vs. 0.14±0.38 (p=0.54 vs. control, p=0.08 vs. PAH)). Lung injury score was similar among groups (control vs. PAH vs. PAH+carvedilol 0.14±0.03 vs. 0.15±0.04 (p=0.62 vs. control) vs. 0.16±0.04 (p=0.32 vs. control, p=0.66 vs. PAH).

Myocyte hypertrophy

LV and RV cardiomyocyte diameters increased in the PAH group vs. controls (RV 21±3 vs. 33±4 μm, p<0.001; LV 22±3 vs. 26±3 μm, p<0.01; Fig. 4a, c). Carvedilol decreased RV cardiomyocyte diameter vs. PAH animals (33±4 vs. 30±4 μm, p<0.05; Fig. 4c). LV cardiomyocyte diameter was unchanged.

Interstitial fibrosis

RV (5.9±1.1 vs. 13.4±6.5 %, p<0.001) and LV (4.6±1.5 vs. 7.9±4.2 %, p<0.01) collagen was increased in PAH vs. controls (Fig. 4b, d). Carvedilol reduced collagen in both RV (13.4±6.5 vs. 5.5±2.7 %, p<0.001) and LV (7.9±4.2 vs. 4±2 %, p<0.001) vs. PAH (Fig. 4b, d).

Fibrosis signaling

RV and LV TGFβ1 and CTGF protein expression were significantly increased in PAH vs. controls (Figs. 5 and 6a, b). RV TGFβ1 and CTGF protein levels decreased with carvedilol vs. PAH and trended to decrease in the LV. Figure 6c–f shows downstream TGFβ1-CTGF fibrosis signaling and apoptosis proteins (Fig. 6g–h). RV and LV Smad 2/3 and p38 were increased in PAH and decreased with carvedilol (Fig. 6c, e). RV Smad4 was increased in PAH and decreased with carvedilol. LV Smad4 was similar among groups (Fig. 6d).

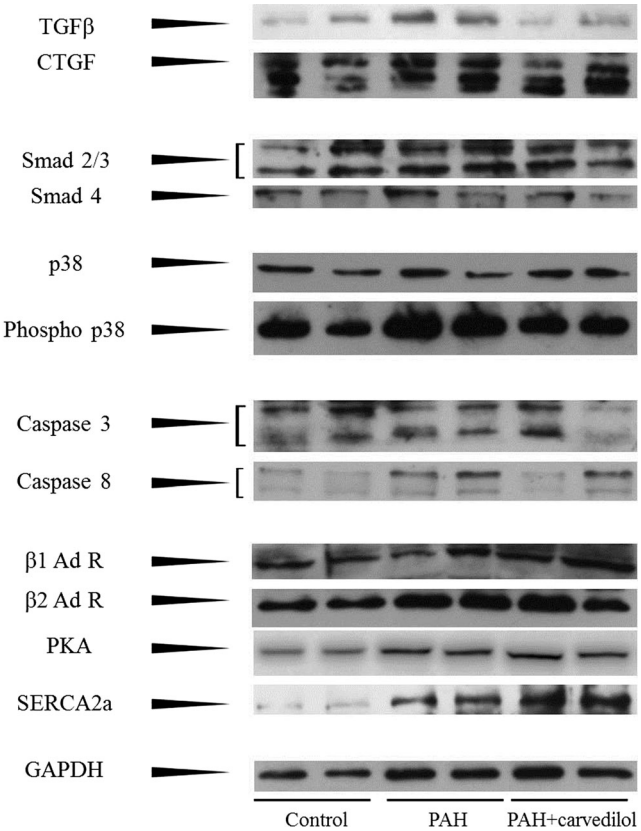

Fig. 5 Carvedilol ameliorates pro-fibrotic and apoptosis signaling induced by pulmonary arterial hypertension. Western blots of right ventricular protein expression of transforming growth factor beta 1 (*TGFβ1*), connective tissue growth factor (*CTGF*), mothers against decapentaplegic (*Smad 2/3*, *Smad 4*), p38, phospho p38, caspase 3, caspase 8, β1 adrenergic receptor (*AdR*), β2 adrenergic receptor (*AdR*), protein kinase A (*PKA*) and sarcoplasmic reticulum Ca^{2+} ATPase (*SERCA2a*). Glyceraldehyde 3-phosphate dehydrogenase (GAPDH) is the internal control (n=2), pulmonary arterial hypertension (PAH) (n=2), PAH+carvedilol rats (n=2)

Apoptosis

RV caspase-8 expression was increased in PAH and decreased with carvedilol. Increased LV caspase-8 did not reach statistical difference in PAH, but carvedilol decreased its expression vs. PAH (Fig. 6h). RV and LV caspase-3 were similar among groups (Fig. 6g).

Extracellular matrix remodeling

RV and LV MMP-2 and MMP-9 were increased in PAH vs. controls and reduced with carvedilol (Fig. 6i, j).

β-adrenergic receptors and calcium handling

RV β1 and β2 adrenergic receptors were increased in PAH+carvedilol vs. PAH (Fig. 7a, b). RV PKA expression was increased in PAH vs. controls (Fig. 7c). RV SERCA2a expression

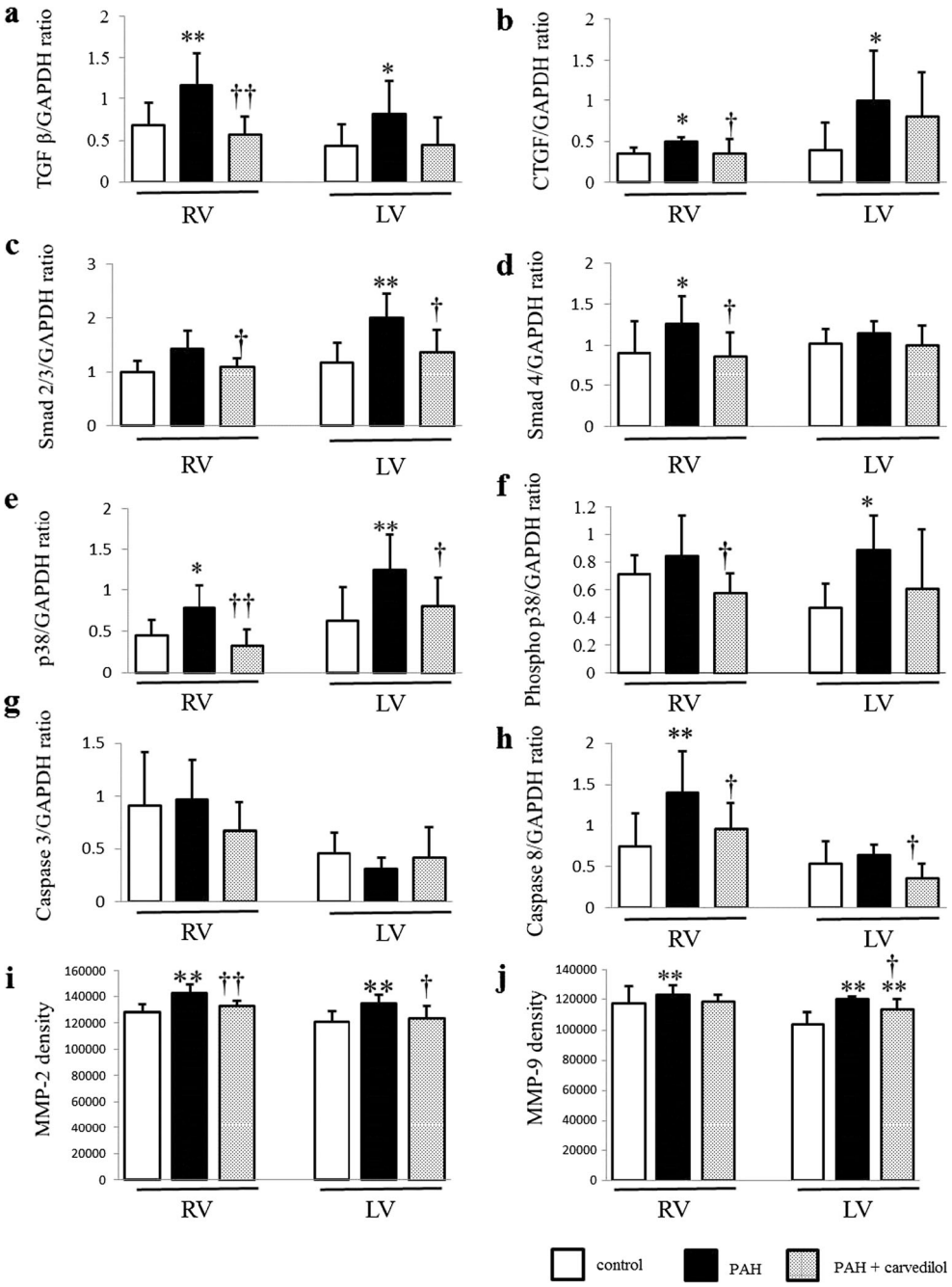

Fig. 6 Carvedilol ameliorates right and left ventricular pro-fibrotic signaling and extracellular matrix remodeling induced by pulmonary arterial hypertension. Ratio of TGFβ1 to glyceraldehyde 3-phosphate dehydrogenase (*GAPDH*) expression (**a**), ratio of connective tissue growth factor (*CTGF*) to GAPDH expression (**b**). Ratio of Smad 2/3 to GAPDH expression (**c**), ratio of Smad4 to GAPDH expression (**d**), ratio of p38 to GAPDH expression (**e**), ratio of phospho-p38 to GAPDH expression (**f**), ratio of caspase-3 to GAPDH expression (**g**), and ratio of caspase-8 to GAPDH expression (**h**) in both ventricles obtained from control (n=8), pulmonary arterial hypertension (*PAH*) (n=7), and PAH+ carvedilol groups (n=8). Ventricular matrix metalloproteinase (MMP)-2 (panel **i**) and MMP-9 (panel **j**) expression in control, pulmonary arterial hypertension (PAH), and PAH+carvedilol groups is quantified for the right and left ventricles. *p<0.05, **p<0.01 vs. control group, †p<0.05, ††p<0.01 vs. PAH group

was increased in PAH+carvedilol (Figs. 7d and 8). LV β1, β2 receptors, PKA, and SERCA2a were similar among groups.

Discussion

We demonstrate beneficial effects of carvedilol on ventricular-ventricular interactions and biventricular TGFβ1-CTGF signaling, fibrosis, and function, despite persistently severe RV afterload.

MRI studies [17] and our own experimental work suggest that fibrosis is central to adverse ventricular-ventricular interactions and biventricular dysfunction in increased RV afterload [6]. Cardiac hypertrophy due to pressure overload is associated with increased ECM deposition, cardiac fibroblast proliferation, and myocyte hypertrophy [18]; with TGFβ1 and CTGF playing central roles. We found improved RV and LV cardiomyocyte hypertrophy with carvedilol despite persistent RV afterload. TGFβ1 is upregulated in hypertrophied myocardium and its expression correlates with fibrosis in the pressure-loaded human heart [19]. We recently

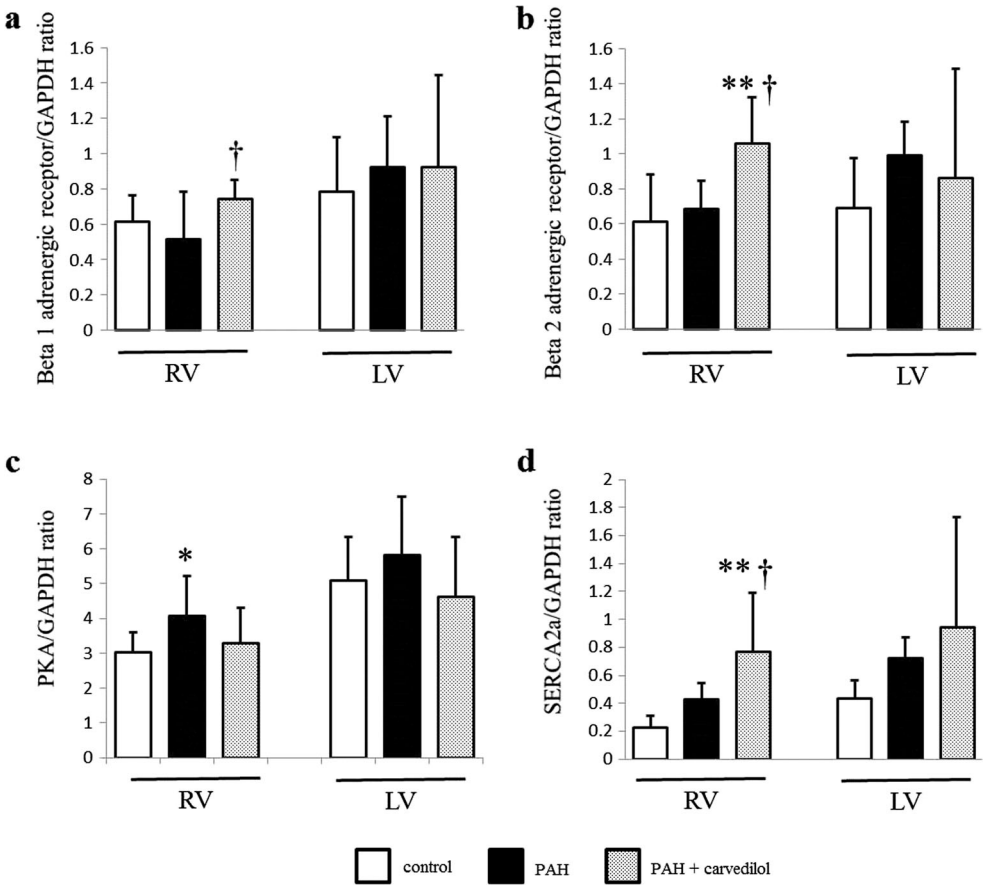

Fig. 7 Ratio of β1 adrenergic receptor to glyceraldehyde 3-phosphate dehydrogenase (*GAPDH*) expression (**a**), ratio of β2 adrenergic receptor to GAPDH expression (**b**), ratio of protein kinase A (*PKA*) to GAPDH expression (**c**), and ratio of cardiac sarcoplasmic reticulum Ca^{2+} ATPase (*SERCA2a*) to GAPDH expression (**d**) in both ventricles obtained from control (n=8), pulmonary arterial hypertension (*PAH*) (n=7), and PAH+carvedilol groups (n=8). **p<0.01 vs. control group, †p<0.05 vs. PAH group

demonstrated that angiotensin receptor blockade reduces biventricular fibrosis in isolated RV afterload through amelioration of TGFβ1-CTGF signaling [5]. Our current results support a central role for abrogation of biventricular TGFβ1 signaling in RV afterload by carvedilol, as evidenced by reduced biventricular collagen content, TGFβ1 expression, and downstream fibrosis signaling. Although reduced hypertrophy in the pressure-loaded RV has been reported with adrenergic blockade, the mechanisms remains elusive [8]. Carvedilol may alter gene expression controlling RV and LV hypertrophy [20]. In the current study, RV and LV TGFβ1 and CTGF were upregulated in the PAH group and downregulated with addition of carvedilol. CTGF acts downstream of TGFβ1 to promote cardiac remodeling and fibrosis through Smad signaling [21] or through p38-mitogen-activated-protein kinase (p38-MAPK) [22]. Our results suggest that Smad and p38-MAPK signaling, as well as MMPs play a role in RV afterload-induced biventricular hypertrophy and fibrosis; and that carvedilol attenuates these pathways.

ECM remodeling and MMPs contribute to cardiac hypertrophy and failure [23]. MMP-2 and MMP-9 are upregulated in monocrotaline-PAH RV hypertrophy and in isolated RV afterload by pulmonary artery banding [23]. Indeed, we found increased biventricular MMP-2 and MMP-9 expression in PAH which was reduced by carvedilol, together with decreased TGFβ1-CTGF signaling. Likewise, TGFβ1 promotes cardiac fibroblast differentiation via MMP-2 [24]. Hence, carvedilol may reduce fibrosis and ECM remodeling through several mechanisms [25]. Similarly, apoptosis promotes biventricular injury in acute and chronic RV failure and at least in the RV appears to be improved by carvedilol [26].

Histologic improvements with carvedilol were associated with improved RV and LV function. Given that beta-blockers are currently contraindicated in PAH due to concerns for reduced cardiac output, our results demonstrating increased cardiac output, despite lower heart rate, are important in association with improved load-independent measures of RV and LV contractility and "gold-standard" measures of RV and LV diastolic relaxation. These results extend prior data that only investigated TAPSE to assess RV systolic function [8].

Beta-blockers improve remodeling, function, and mortality in LV failure. However, little is known about their effects in RV afterload. In our study, carvedilol improved not only RV but also LV tissue injury and fibrosis. These improvements were associated with improved LV pump and myocardial performance.

We recently reported on the *S*/*D* ratio to measure ventricular-ventricular interactions in children with PAH demonstrating that a higher *S*/*D* ratio, an index that worsens at higher heart rates, is associated with increased mortality [4]. We now demonstrate improved RV and LV *S*/*D* ratios, suggesting that carvedilol,

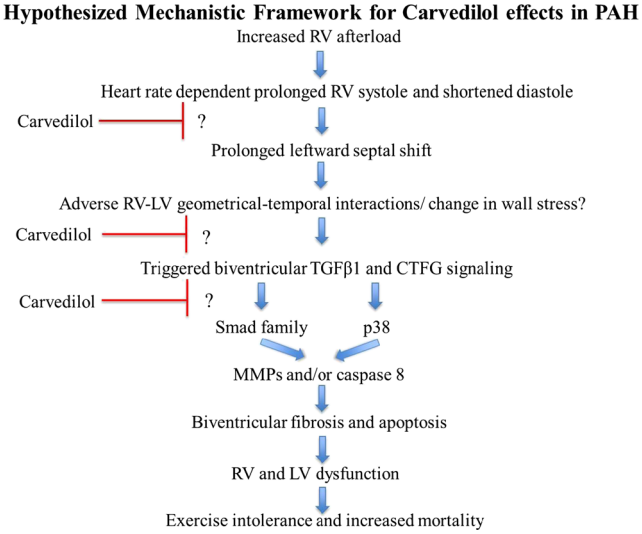

Fig. 8 Hypothesized mechanistic framework and rationale for carvedilol in increased right ventricular (RV) afterload. Based on previous investigations, we hypothesize that increased RV afterload leads to a relative prolongation of RV systolic duration and shortened diastolic duration. This phenomenon contributes to RV dysfunction and worsens with increasing heart rates. The prolonged RV systole also leads to adverse ventricular-ventricular interactions with leftward septal shift and a possible change in LV geometry with resultant increased wall stress. We hypothesize that this triggers biventricular TGFβ1 and CTGF signaling leading to biventricular fibrosis and apoptosis, ventricular dysfunction, worsened hemodynamics, and reduced exercise tolerance and survival. We postulate that carvedilol may act through a heart rate effect to change the systolic-diastolic duration and hence biventricular function as well as interactions. Carvedilol may also reduce ventricular wall stress and reduce pro-fibrotic signaling thereby improving cardiac fibrosis and function

either through direct effects, or secondary to lower heart rate, improves biventricular function and ventricular-ventricular interactions. Improved *S/D* ratio was associated with improved diastolic parameters in both ventricles.

Increased RV afterload leads not only to decreased RV strain [11] but also reduced LV strain; both improved with carvedilol. Pulmonary pressures were persistently high with carvedilol and not different between groups. Likewise, lung injury was comparable between groups; implying that carvedilol effects on increased stroke volume, and cardiac index were independent of pulmonary effects. This was supported by worsening of load-independent measures of LV and RV contractility in PAH rats and improvement with carvedilol. Hence, although carvedilol may potentially reduce monocrotaline-induced myocarditis, we observed no substantial inflammation in all groups. Likewise, lung injury was low and similar between PAH and PAH+carvedilol. Therefore, carvedilol effects were unlikely due to lung effects or myocarditis. Likewise, in our prior work using a rabbit pulmonary artery band model, we observed both RV and LV fibrosis, supporting the notion that LV changes seen in the current experiments were not induced by monocrotaline. While we did not delineate what exactly triggers upregulated LV TGFβ1-CTGF signaling, altered hemodynamics, geometrical changes, increased wall stress, paracrine, and even endocrine signaling are possibilities that require further investigation.

β-adrenergic receptor expression and intracellular calcium handling

Given improved biventricular diastolic function and *S/D* ratio, we investigated PKA and SERCA2a. Carvedilol upregulated RV SERCA2a expression in PAH animals with similar trends in the LV. SERCA2a plays a central role in myocardial contractility and relaxation [27]. Downregulated SERCA2a in failing myocardium impairs intracellular calcium cycling and systolic and diastolic dysfunction. This may contribute to the beneficial effects of carvedilol despite persistent PAH.

We also demonstrated that carvedilol upregulated RV β1/β2 adrenergic receptor expression, although interestingly not in the LV. While increased adrenergic receptor expression is part of the fetal gene reactivation program in response to RV afterload, some studies have reported reduced β1-adrenergic receptors in PAH patients and animal models [8]. Increased β-adrenergic receptor expression likely stems from the β-blockade itself. PKA expression, downstream of β-adrenergic receptors and upstream of SERCA2a, was upregulated in the RV in PAH, although not in the LV [27]. Whether carvedilol exerts its effects through direct interaction of G-protein receptor signaling, possibly PKA, with TGFβ1-CTGF molecular signaling, or whether its effects are secondary to altered cardiac mechanics or hemodynamics requires further investigation. Bogaard et al. found increased protein kinase G (PKG) activity following carvedilol in pulmonary hypertensive rats [8] while we found increased smad signaling and increased PKA in PAH rats, and a trend to reduction with carvedilol. G-protein coupled receptor signaling has been reported to interact with TGFβ1 signaling independent of smads [28]. Whether these G-protein smad-independent effects are important in our model requires further investigation.

We characterized the β-adrenergic response after sustained carvedilol treatment by investigating acute hemodynamic responses to dobutamine and esmolol. These experiments demonstrated intact response to beta stimulation and blockade. Therefore, carvedilol-treated animals maintain an intact beta-adrenergic response consistent with upregulation of β-adrenergic receptors. Both groups showed a similar increase in contractility to dobutamine, despite the relatively higher upregulation of beta-1 receptors in the carvedilol group. This may be due to a relatively modest increase in β-1 receptors in the RV only, or possibly due to a concomitant upregulation of β-2 receptors.

Clinical implications

Carvedilol lowers heart rate and hence the concern for low cardiac output in PAH patients. However, we demonstrated that the lower heart rate improves the *S*/*D* ratio and hence ventricular-ventricular interactions; with a concomitant increase in cardiac index. Additionally, carvedilol upregulated RV β-adrenergic receptors and did not blunt the acute β-adrenergic response. Indeed RV and LV contractility were improved with carvedilol and cardiac output preserved. Thus, clinical trials to evaluate this in a controlled setting seem warranted.

Study limitations

In an in vivo setting, we could not evaluate whether beneficial LV effects were secondary to RV effects. However, the complexities of the in vivo model are important, certainly for ventricular-ventricular interactions. Although we studied TGFβ1-CTGF fibrosis signaling in detail, further delineation of downstream beta-adrenergic specific signaling warrants investigation. Likewise, whether therapeutic effects of beta-blockade are through heart-rate modulation or through other adrenergic effects requires further study.

In conclusion, despite persistently severe RV afterload, carvedilol improves biventricular TGFβ1-CTGF signaling, fibrosis, ECM remodeling, and apoptosis. It also improved biventricular function and exercise endurance.

Acknowledgments The Canadian Institutes of Health Research supported this research.

Conflicts of interest The authors declare that they have no conflicts of interest.

References

1. Kitaori K, He H, Ayres SM, Kawata M, Cowan DB, Friehs I, del Nido PJ, McGowan FX (2009) Development of left ventricular diastolic dysfunction with preservation of ejection fraction during progression of infant right ventricular hypertrophy. Circ Heart Fail 2: 599–607
2. Handoko ML, de Man FS, Allaart CP, Paulus WJ, Westerhof N, Vonk-Noordegraaf A (2010) Perspectives on novel therapeutic strategies for right heart failure in pulmonary arterial hypertension: lessons from the left heart. Eur Respir Rev 19:72–82
3. Gan CT, Lankhaar JW, Marcus JT, Westerhof N, Marques KM, Bronzwaer JG, Boonstra A, Postmus PE, Vonk-Noordegraaf A (2006) Impaired left ventricular filling due to right-to-left ventricular interaction in patients with pulmonary arterial hypertension. Am J Physiol Heart Circ Physiol 290:H1528–H1533
4. Alkon J, Humpl T, Manlhiot C, McCrindle BW, Reyes JT, Friedberg MK (2010) Usefulness of the right ventricular systolic to diastolic duration ratio to predict functional capacity and survival in children with pulmonary arterial hypertension. Am J Cardiol 106:430–436
5. Friedberg MK, Cho MY, Li J, Assad RS, Sun M, Rohailla S, Honjo O, Apitz C, Redington AN (2013) Adverse biventricular remodeling in isolated right ventricular hypertension is mediated by increased TGFbeta1 signaling and is abrogated by angiotensin receptor blockade. Am J Respir Cell Mol Biol 49:1019–1028
6. Apitz C, Honjo O, Humpl T, Li J, Assad RS, Cho MY, Hong J, Friedberg MK, Redington AN (2012) Biventricular structural and functional responses to aortic constriction in a rabbit model of chronic right ventricular pressure overload. J Thoracic Cardiovasc Surg 144:1494–1501
7. Nootens M, Kaufmann E, Rector T, Toher C, Judd D, Francis GS, Rich S (1995) Neurohormonal activation in patients with right ventricular failure from pulmonary hypertension: relation to hemodynamic variables and endothelin levels. J Am Coll Cardiol 26:1581–1585
8. Bogaard HJ, Natarajan R, Mizuno S, Abbate A, Chang PJ, Chau VQ, Hoke NN, Kraskauskas D, Kasper M, Salloum FN et al (2010) Adrenergic receptor blockade reverses right heart remodeling and dysfunction in pulmonary hypertensive rats. Am J Respir Crit Care Med 82:652–660
9. Tei C, Dujardin KS, Hodge DO, Bailey KR, McGoon MD, Tajik AJ, Seward SB (1996) Doppler echocardiographic index for assessment of global right ventricular function. J Am Soc Echocardiogr 9:838–847
10. Duan Y, Harada K, Wu W, Ishii H, Takada G (2008) Correlation between right ventricular Tei index by tissue Doppler imaging and pulsed Doppler imaging in fetuses. Pediatr Cardiol 29:739–743
11. Fukuda Y, Tanaka H, Sugiyama D, Ryo K, Onishi T, Fukuya H, Nogami M, Ohno Y, Emoto N, Kawai H et al (2011) Utility of right ventricular free wall speckle-tracking strain for evaluation of right ventricular performance in patients with pulmonary hypertension. J Am Soc Echocardiogr 24:1101–1108
12. Koopman LP, Slorach C, Manlhiot C, McCrindle BW, Jaeggi ET, Mertens L, Friedberg MK (2011) Assessment of myocardial deformation in children using Digital Imaging and Communications in Medicine (DICOM) data and vendor independent speckle tracking software. J Am Soc Echocardiogr 24:37–44
13. Hessel MH, Steendijk P, den Adel B, Schutte CI, van der Laarse A (2006) Characterization of right ventricular function after monocrotaline-induced pulmonary hypertension in the intact rat. Am J Physiol Heart Circ Physiol 291:H2424–H2430
14. Matute-Bello G, Downey G, Moore BB, Groshong SD, Matthay MA, Slutsky AS, Kuebler WM (2011) An official American Thoracic Society workshop report: features and measurements of experimental acute lung injury in animals. Am J Respir Cell Mol Biol 44:725–738
15. van Heeswijk RB, De Blois J, Kania G, Gonzales C, Blyszczuk P, Stuber M, Eriksson U, Schwitter J (2013) Selective in vivo visualization of immune-cell infiltration in a mouse model of autoimmune myocarditis by fluorine-19 cardiac magnetic resonance. Circ Cardiovasc Imaging 6:277–284
16. Sun M, Opavsky MA, Stewart DJ, Rabinovitch M, Dawood F, Wen WH, Liu PP (2003) Temporal response and localization of integrins beta1 and beta3 in the heart after myocardial infarction: regulation by cytokines. Circulation 107:1046–1052
17. Shehata ML, Lossnitzer D, Skrok J, Boyce D, Lechtzin N, Mathai SC, Girgis RE, Osman N, Lima JA, Bluemke DA et al (2011) Myocardial delayed enhancement in pulmonary hypertension: pulmonary hemodynamics, right ventricular function, and remodeling. AJR Am J Roentgenol 196:87–94
18. Frey N, Olson EN (2003) Cardiac hypertrophy: the good, the bad, and the ugly. Annu Rev Physiol 65:45–79
19. Villarreal FJ, Dillmann WH (1992) Cardiac hypertrophy-induced changes in mRNA levels for TGF-beta 1, fibronectin, and collagen. Am J Physiol 262:H1861–H1866

20. Drake JI, Gomez-Arroyo J, Dumur CI, Kraskauskas D, Natarajan R, Bogaard HJ, Fawcett P, Voelkel NF (2013) Chronic carvedilol treatment partially reverses the right ventricular failure transcriptional profile in experimental pulmonary hypertension. Physiol Genomics 45:449–461
21. Mori T, Kawara S, Shinozaki M, Hayashi N, Kakinuma T, Igarashi A, Takigawa M, Nakanishi T, Takehara K (1999) Role and interaction of connective tissue growth factor with transforming growth factor-beta in persistent fibrosis: a mouse fibrosis model. J Cell Physiol 181:153–159
22. Mu Y, Gudey SK, Landstrom M (2012) Non-Smad signaling pathways. Cell Tissue Res 347:11–20
23. Okada M, Kikuzuki R, Harada T, Hori Y, Yamawaki H, Hara Y (2008) Captopril attenuates matrix metalloproteinase-2 and -9 in monocrotaline-induced right ventricular hypertrophy in rats. J Pharmacol Sci 108:487–494
24. Stawowy P, Margeta C, Kallisch H, Seidah NG, Chretien M, Fleck E, Graf K (2004) Regulation of matrix metalloproteinase MT1-MMP/MMP-2 in cardiac fibroblasts by TGF-beta1 involves furin-convertase. Cardiovasc Res 63:87–97
25. Zhang YJ, Xiang MX, San J, Cheng G, Wang SS (2006) Effect of matrine and carvedilol on collagen and MMPs activity of hypertrophy myocardium induced by pressure overload. J Zhejiang Univ Sci B 7:245–250
26. Dewachter C, Dewachter L, Rondelet B, Fesler P, Brimioulle S, Kerbaul F, Naeije R (2010) Activation of apoptotic pathways in experimental acute afterload-induced right ventricular failure. Crit Care Med 38:1405–1413
27. Periasamy M, Bhupathy P, Babu GJ (2008) Regulation of sarcoplasmic reticulum Ca2+ ATPase pump expression and its relevance to cardiac muscle physiology and pathology. Cardiovasc Res 77:265–273
28. Derynck R, Zhang YE (2003) Smad-dependent and Smad-independent pathways in TGF-beta family signaling. Nature 425:577–584